RSC Advances

PAPER

View Article Online
View Journal | View Issue

Check for updates

Cite this: *RSC Adv.*, 2023, **13**, 23402

The alkoxy radical polymerization of *N*-vinylpyrrolidone in organic solvents: theoretical insight into the mechanism and kinetics†

Quan V. Vo, *[a] Truong Le Bich Tram,*[b] Loc Phuoc Hoang, *[c] Nguyen Thi Hoa[a] and Adam Mechler [d]

Poly(*N*-vinylpyrrolidone) (**PVP**) is a polymer with many applications in cosmetic, pharmaceutical, and biomedical formulations due to its minimal toxicity. **PVP** can be synthesized through radical polymerization in organic solvents; this well-known industrial process is thoroughly characterized experimentally, however, quantum chemical modeling of the process is scarce: the mechanism and kinetics have not been thoroughly investigated yet. In this work, the mechanism and kinetics of the alkoxy radical polymerization of *N*-vinylpyrrolidone in organic solvents, namely isopropanol (**IP**) and toluene (**TL**), were successfully modeled by computational chemistry. The initiator radicals di-*tert*-butyl peroxide (**TBO**$^{\bullet}$) and dicumyl peroxide (**CMO**$^{\bullet}$) as well as the solvents isopropanol and toluene, were shown to be capable of assisting in the initiation reactions. The rate constant was influenced by the combination of initiators and solvent and the values of the rate constant of propagation were approximately 10^{1}–10^{3} M^{-1} s^{-1}. The radical polymerization of **NVP** with dicumyl peroxide as an initiator was comparable to that of di-*tert*-butyl peroxide in all of the examined organic solvents, whereas the solvents had less of an effect.

Received 7th June 2023
Accepted 31st July 2023

DOI: 10.1039/d3ra03820c

rsc.li/rsc-advances

Open Access Article. Published on 04 August 2023. Downloaded on 2/16/2026 2:18:28 AM.
This article is licensed under a Creative Commons Attribution 3.0 Unported Licence.

1. Introduction

In cosmetic, pharmaceutical, and biomedical formulations, poly(*N*-vinylpyrrolidone) (PVP) is frequently used because of its biocompatibility, biodegradability, potent complexing ability, and superior film-forming qualities.[1] It is a nonionic, amorphous polymer that is soluble in both organic solvents and water.[2,3] In medical formulations, it can be found in a wide range of granules, tablets, soft gelatin capsules, hydrogels, films, palettes, and other medical device coatings.[2]

N-Vinylpyrrolidone (**NVP**, Fig. 1) is typically polymerized in an aqueous solution with hydrogen peroxide as initiator, or in organic solvents such as isopropanol (**IP**) or toluene (**TL**) with organic peroxides such as di-*tert*-butyl peroxide $(\mathbf{TBO})_2$ or dicumyl peroxide $(\mathbf{CMO})_2$ as initiators (Fig. 1).[4–6] The radicals in the organic solvent, such as alcohols or toluene, act as the reaction's initiators when polymerization is carried out with organic peroxides like $(\mathbf{TBO})_2$ or $(\mathbf{CMO})_2$. It was discovered that the PVP made in organic solutions was more stable, and no pyrrolidone impurity production was seen, unlike when polymerization was carried out in aqueous solvents with H_2O_2 as an initiator.[5] The polymerization of **NVP** in polar media by radicals *i.e.* HO$^{\bullet}$ garnered some attention in the literature,[7–16] where the mechanism and kinetics have been investigated.[10,11,16] However, the alkoxy radical polymerization in organic solvents was not studied with the same fervor, despite of the fact that the PVP made in organic solutions was more stable and no pyrrolidone impurity production was seen.[4,5]

In the field of radical reactions and polymerizations, the *in silico* approach has gained popularity recently as a technique for analyzing the kinetics and mechanism of radical processes. While using the least amount of resources and time possible, new techniques and procedures create dependable data.[17–30] In this study, we use a well-established method based on quantum chemistry,[16,31,32] to investigate the alkoxy radical (**TBO**$^{\bullet}$ and **CMO**$^{\bullet}$) polymerization of *N*-vinylpyrrolidone in **IP** and **TL**.

2. Computational details

The kinetic calculations were performed using the quantum mechanics-based test for the overall free radical scavenging activity (QM-ORSA) technique,[31] which is directly applicable given the chemical analogy between all radical reactions.[17,33,34]

[a]*The University of Danang—University of Technology and Education, Danang 550000, Vietnam. E-mail: vvquan@ute.udn.vn; vovanquan1980@gmail.com*

[b]*Department of Science-Technology and Environment, The University of Danang, Danang 550000, Vietnam. E-mail: tlbtram@ac.udn.vn*

[c]*Quang Tri Teacher Training College, Dong Ha, Quang Tri, 520000, Vietnam. E-mail: loc_hp@qtttc.edu.vn*

[d]*Department of Biochemistry and Chemistry, La Trobe University, Victoria 3086, Australia*

† Electronic supplementary information (ESI) available. See DOI: https://doi.org/10.1039/d3ra03820c

© 2023 The Author(s). Published by the Royal Society of Chemistry

Open Access Article. Published on 04 August 2023. Downloaded on 2/16/2026 2:18:28 AM.
This article is licensed under a Creative Commons Attribution 3.0 Unported Licence.

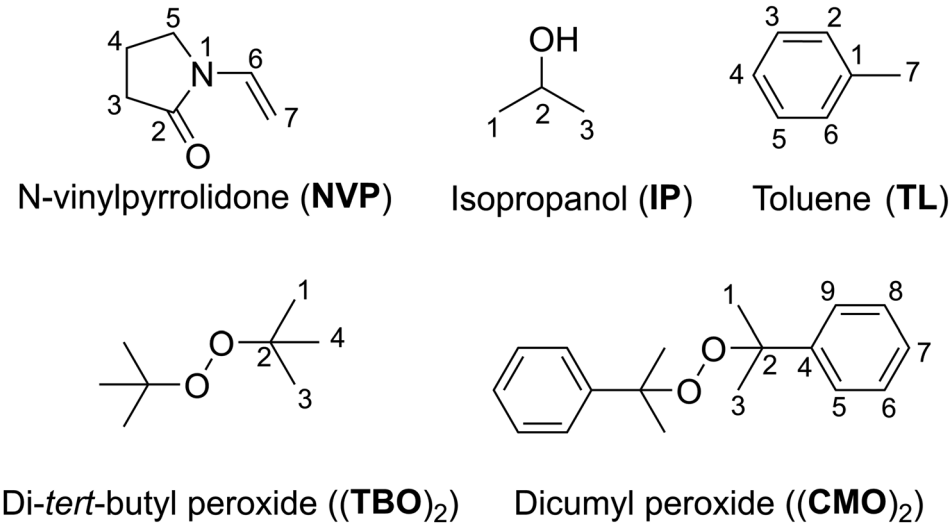

Fig. 1 Structure and numbering of NVP, $(TBO)_2$, $(CMO)_2$, IP and TL.

Fig. 2 The initiation reaction of the TBO•/CMO• in isopropanol (IP) and toluene (TL) (R:TB, CM; R_1•:TBO•, CMO•, IP•, TL•).

The rate constant (k) was determined by applying eqn (1) to the 1 M standard state at 298.15 K and the transition state theory (TST).[35–39]

$$k = \sigma\kappa \frac{k_B T}{h} e^{-(\Delta G^{\neq})/RT} \quad (1)$$

where σ is the reaction symmetry number,[40,41] κ stands for tunneling corrections that were calculated using Eckart barrier,[42] k_B is the Boltzmann constant, h is the Planck constant and $\Delta G^{\neq}$ is Gibbs free energy of activation.

Those rate constants near the diffusion limit were modified.[33] To obtain the apparent rate constants (k_{app}) for an irreversible bimolecular diffusion-controlled reaction in solvents at 298.15 K, the Collins–Kimball theory[43] and the literature were consulted to determine the steady-state Smoluchowski rate constant (k_D).[33,44]

$$k_{app} = \frac{k_{TST} k_D}{k_{TST} + k_D} \quad (2)$$

$$k_D = 4\pi R_{AB} D_{AB} N_A \quad (3)$$

$D_{AB} = D_A + D_B$, where D_A or D_B is the mutual diffusion coefficient of A and B as calculated using the Stokes–Einstein formulation (4).[43,45–47]

$$D_{A\text{ or }B} = \frac{k_B T}{6\pi\eta a_{A\text{ or }B}} \quad (4)$$

η is the viscosity of the solvents and a is the radius of the solute that was obtained in Gaussian calculations. The viscosity of isopropanol is 20.4×10^{-4} Pa s and that of toluene is 5.60×10^{-4} Pa s. Identifiable transition states had a single imaginary frequency. To ensure that each transition state is accurately associated with the pre- and post-complexes, calculations with intrinsic coordinates were conducted.

All computations for this investigation were performed utilizing the M06-2X/6-311++G(d,p) method from the Gaussian 16 software package.[48] This model chemistry yields the most precise thermodynamics and kinetics outcomes.[49–53] It is frequently used to assess the radical reactions with small errors in comparison to experimental data (k_{calc}/k_{exp} ratio = 0.2–2.9).[16,32,33,38,54–56] The SMD method was used to model the effects of isopropanol and toluene.[57] AIM2000 software was used to conduct atom-in-molecule (AIM) analysis at the M06-2X/6-311++G(d,p) level.[58,59]

3. Results and discussion

3.1 Initiation reactions of TBO•/CMO• in the organic solvents

To investigate the initiation reaction of the polymerization utilizing organic peroxides such as di-*tert*-butyl peroxide

Table 1 The calculated values of the ΔG° for the IP/TL + TBO•/CMO• reactions in the IP and TL

Solvents	Mechanisms	Positions	TBO•	CMO•
IP	FHT	C1–H	−5.2	−5.4
		C2–H	−13.8	−14.0
		O2–H	−0.8	−1.0
TL	FHT	C7–H	−13.0	−13.4
	RAF	C1	11.3	12.6
		C2	10.9	12.2
		C3	9.4	10.5
		C4	8.5	9.4

Open Access Article. Published on 04 August 2023. Downloaded on 2/16/2026 2:18:28 AM.
This article is licensed under a Creative Commons Attribution 3.0 Unported Licence.

Table 2 Calculated $\Delta G^{\neq}$ (*k*cal mol^{-1}), tunneling corrections (κ), rate constants (k_{app}, k_r, and $k_{overall}$ M^{-1} s^{-1}) and branching ratios (Γ,%) for the IP/TL + TBO$^{\bullet}$/CMO$^{\bullet}$ reactions[a]

			TBO$^{\bullet}$				CMO$^{\bullet}$			
Solvents	Mechanisms		$\Delta G^{\neq}$	κ	k_{app}	Γ	$\Delta G^{\neq}$	κ	k_{app}	Γ
IP	FHT	C1–H	16.7	13.0	2.70×10^2	1.2	15.2	8.4	2.10×10^3	2.7
		C2–H	11.9	2.0	2.30×10^4	98.5	10.9	1.3	7.60×10^4	96.8
		O2–H	18.3	361.9	8.00×10^1	0.3	16.7	107.9	3.90×10^2	0.5
	$k_{overall}$				2.34×10^4				7.85×10^4	
TL	FHT	C7–H	14.7	8.0	8.90×10^2		16.4	7.5	4.60×10^1	

[a] $k_{overall} = \sum k_{app}$; $\Gamma = k_{app} \times 100/k_{overall}$

((**TBO**)$_2$) or dicumyl peroxide ((**CMO**)$_2$) in organic solvents such as **IP**, or **TL**, all potential radical reactions could occur following the reactions 5–9 (Fig. 2). The alkoxy radicals are formed by heating peroxides in accordance with reaction 5, while the **TBO**$^{\bullet}$, **CMO**$^{\bullet}$ radicals can react with solvents or **NVP** at possible reactions, *i.e.* the formal hydrogen transfer (FHT, reactions 6, 7, and Table 1) and the radical adduct formation (RAF, reaction 8, 9 and Table 1). As shown in Table 1, the FHT mechanism for the **IP**/**TL** + **TBO**$^{\bullet}$/**CMO**$^{\bullet}$ reactions is thermodynamically spontaneous (ΔG° = −14.0 to −0.8 kcal mol^{-1}), whereas the RAF mechanism is thermodynamically nonspontaneous ($\Delta G^{\circ} > 0$) for all of the studied solvents and radicals. Thus the kinetics of the **IP**/**TL** + **TBO**$^{\bullet}$/**CMO**$^{\bullet}$ reactions were computed and presented in Table 2 and Fig. 3.

As shown in Table 2, the H-abstraction at the C2–H bond defined the **IP** + **TBO**$^{\bullet}$/**CMO**$^{\bullet}$ reactions with the $k_{app} = 2.30 \times 10^4$ (Γ = 98.5%) and 7.60×10^4 (Γ = 96.8%) M^{-1} s^{-1} for the **TBO**$^{\bullet}$ and **CMO**$^{\bullet}$ radicals, respectively, whereas the FHT reaction of the O2–H bond contributed only 0.3–0.5% in the overall rate constant. Thus the **IP-C2**$^{\bullet}$, which was formed by reaction 6 in

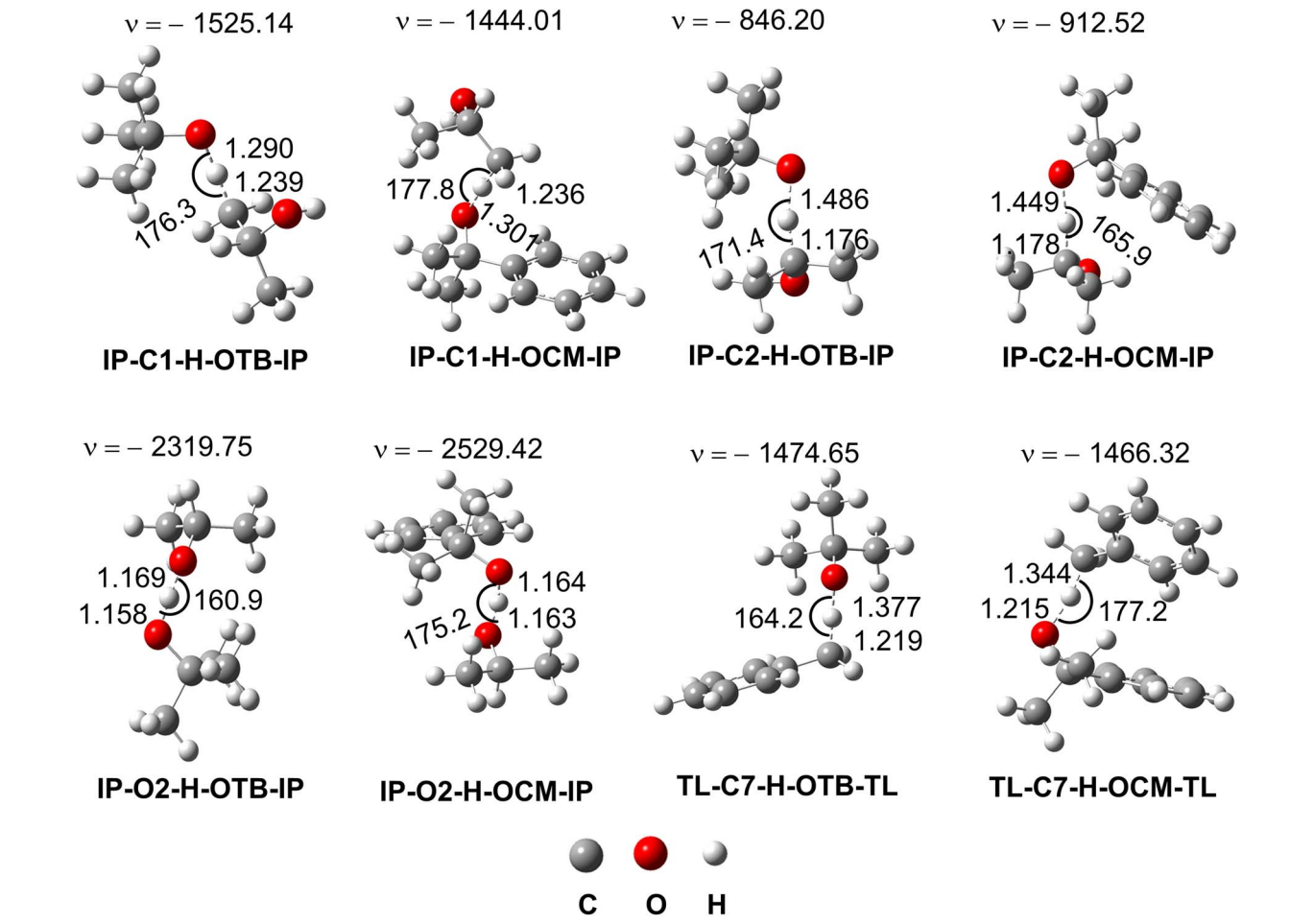

Fig. 3 The transition states of the reactions.

© 2023 The Author(s). Published by the Royal Society of Chemistry

Open Access Article. Published on 04 August 2023. Downloaded on 2/16/2026 2:18:28 AM.
This article is licensed under a Creative Commons Attribution 3.0 Unported Licence.

Table 3 Calculated $\Delta G^{\neq}$ (kcal mol^{-1}), tunneling corrections (κ), rate constants (k_{app}, k_r, and $k_{overall}$ M^{-1} s^{-1}) and branching ratios (Γ,%) for the NVP + IP-C2$^{\bullet}$/TL-C7$^{\bullet}$/TBO$^{\bullet}$/CMO$^{\bullet}$ reactions in the organic solvents

RAD/Sol.	Mechanism		$\Delta G^{\neq}$	κ	k_{app}	Γ
IP-C2$^{\bullet}$/IP	FHT	C3–H	17.7	8.1	5.70	0.1
		C4–H	23.2	22.0	1.40×10^{-3}	0.0
		C5–H	20.8	21.0	7.00×10^{-2}	0.0
	RAF	C6	35.2	1.0	1.10×10^{-13}	0.0
		C7	12.4	1.2	6.20×10^{3}	99.9
	$k_{overall}$				6.21×10^{3}	
TL-C7$^{\bullet}$/TL	FHT	C3–H	24.6	16.0	9.10×10^{-5}	0.0
		C4–H	26.2	21.0	8.80×10^{-6}	0.0
		C5–H	22.4	18.0	4.10×10^{-3}	0.1
	RAF	C6	22.2	1.7	6.20×10^{-4}	0.0
		C7	16.7	1.4	4.50	99.9
	$k_{overall}$				4.50	
TBO$^{\bullet}$/IP	RAF	C7	11.4	1.1	3.10×10^{4}	
CMO$^{\bullet}$/IP			9.7	1.0	5.20×10^{5}	
TBO$^{\bullet}$/TL			12.7	1.2	3.40×10^{3}	
CMO$^{\bullet}$/TL			10.5	1.1	1.50×10^{5}	

the **IP** solvent, is the main radical for the following reactions (*i.e.* 7 and 8). At the same time, the H-abstraction at the C7–H characterized the **TL** + **TBO$^{\bullet}$/CMO$^{\bullet}$** reactions and formed the **TL-C7$^{\bullet}$** radical with $k_{app} = 8.90 \times 10^{2}$ and 4.60×10^{1} M^{-1} s^{-1} for the **TBO$^{\bullet}$** and **CMO$^{\bullet}$** radicals, respectively, however, these are slower than the **IP** + **TBO$^{\bullet}$/CMO$^{\bullet}$** reactions. Thus in the **IP** solution, the **NVP** can react with three main radicals including **IP-C2$^{\bullet}$**, **TBO$^{\bullet}$** and **CMO$^{\bullet}$**, whereas in the **TL** solvent, the **IP-C2$^{\bullet}$** is replaced by the **TL-C7$^{\bullet}$** radical.

To gain insight into the structure of the TSs, the AIM analysis was used to measure the intermolecular contacts (Table S1, Fig. S2, ESI†). It was found that the **TS-IP-C2-H-OTB/OCM-IP** are stabilized by intermolecular contacts at the H5⋯C2, H5⋯O13, (**TBO**)H3⋯O2, (**TBO**)H3⋯H1, (**TBO**)H1⋯C1, (**CMO**)H1⋯O2, (**CMO**)C4⋯H1 and ring critical points (RCPs) at RCP1, RCP2 and RCP3, whereas those of the C1–H are only defined by intermolecular contacts H7⋯C1, H7⋯O13, (**CMO**)C6⋯H1 and RCP1, RCP2. Intermolecular contacts and RCPs define the stability of TSs of the **TS-IP-O2-H-OTB/OCM-IP**; however, the E_{H-B}(O2–H12) values (E_{H-B}(O2–H12) = −87.5 and −90.3 kcal mol^{-1}) are significantly lower than the E_{H-B}(C2–H5) values (E_{H-B}(C2–H5) = −69.3 and −69.9 kcal mol^{-1}). Therefore, the O2–H12 bond may be more difficult to break than the C2–H5 bond when forming the products. This may account for the high stability of **TS-IP-C2-H-OTB/OCM-IP** and the rapid H-abstraction at the C2–H bond. At the TSs of **TL-C7-H** + OTB/OCM reactions, the O16–H13 bond at the **TS-TL-C7-H-OTB** is

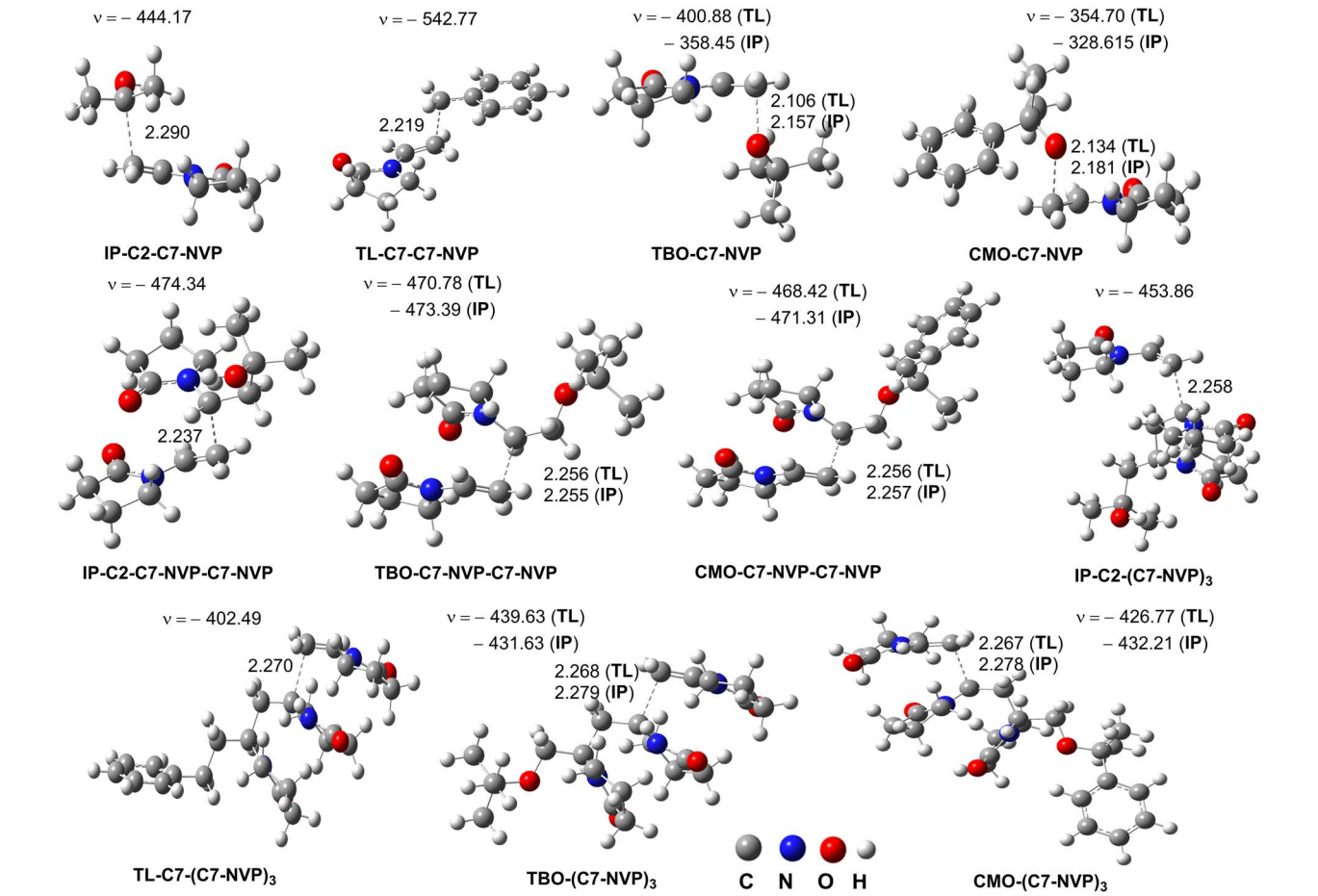

Fig. 4 Selected transition states of the reactions.

Open Access Article. Published on 04 August 2023. Downloaded on 2/16/2026 2:18:28 AM.
This article is licensed under a Creative Commons Attribution 3.0 Unported Licence.

Table 4 Calculated $\Delta G^{\neq}$ (kcal mol^{-1}), tunneling corrections (κ), rate constants (k_p, M^{-1} s^{-1}) the propagation reaction

Reactions	Solvents	$\Delta G^{\neq}$	κ	k_p
IP-C2-C7-NVP$^{\bullet}$ + NVP	**IP**	13.4	1.2	1.20×10^3
TL-C7-C7-NVP$^{\bullet}$ + NVP	**TL**	12.4	1.2	6.10×10^3
TBO-C7-NVP$^{\bullet}$ + NVP	**IP**	13.0	1.2	2.10×10^3
CMO-C7-NVP$^{\bullet}$ + NVP		15.5	1.2	3.30×10^1
TBO-C7-NVP$^{\bullet}$ + NVP	**TL**	13.5	1.2	1.10×10^3
CMO-C7-NVP$^{\bullet}$ + NVP		15.7	1.2	2.50×10^1
IP-C2-C7-NVP-C7-NVP$^{\bullet}$ + NVP	**IP**	16.1	1.2	1.18×10^1
TL-C7-C7-NVP-C7-NVP$^{\bullet}$ + NVP	**TL**	13.7	1.2	6.75×10^2
TBO-C7-NVP-C7-NVP$^{\bullet}$ + NVP	**IP**	12.6	1.1	3.96×10^3
CMO-C7-NVP-C7-NVP$^{\bullet}$ + NVP		14.4	1.0	1.73×10^2
TBO-C7-MVP-C7-NVP$^{\bullet}$ + NVP	**TL**	13.9	1.2	4.82×10^2
CMO-C7-NVP-C7-NVP$^{\bullet}$ + NVP		13.7	1.0	5.63×10^2

more stable than that at the **TS-TL-C7-H-OCM**, which can lead to rapid H-abstraction by the **TBO** radical.

The reaction of **NVP** with alkyl radicals *i.e.* **IP-C2$^{\bullet}$/TL-C7$^{\bullet}$** was first evaluated and the results are presented in Table 3 and Fig. 4. It was found that the RAF reaction at C7 position dominated the **NVP** + **IP-C2$^{\bullet}$/TL-C7$^{\bullet}$** reactions ($\Gamma = 99.9\%$), however the rate constant of the **NVP** + **IP-C2$^{\bullet}$** reaction ($k_{overall} = 6.21 \times 10^3$ M^{-1} s^{-1}) was about 10^3 times faster than that of the **NVP** + **TL-C7$^{\bullet}$** ($k_{overall} = 4.50$ M^{-1} s^{-1}). The other reactions had no contributions to the overall rate constant of the alkyl radical scavenging activity of **NVP**. Thus for the alkoxy radicals *i.e.* **TBO$^{\bullet}$** and **CMO$^{\bullet}$**, the **NVP** + **TBO$^{\bullet}$/CMO$^{\bullet}$** reactions were only focused on the RAF pathway at the C7 position (Table 3 and Fig. 4).

As shown in Table 3, the alkoxy radical reactions of **NVP** in the **IP** solvent were faster than in the **TL** solution. The **NVP** + **TBO$^{\bullet}$/CMO$^{\bullet}$** reactions in the **IP** solution were about 9.1 and 3.5 times faster than those in the **TL** solution for **TBO$^{\bullet}$** and **CMO$^{\bullet}$** respectively. It is important to notice that in the **IP** solution, the formed radical from the solvent (**IP-C2$^{\bullet}$**) can react with **NVP** as fairly fast as the **NVP** + **TBO$^{\bullet}$/CMO$^{\bullet}$** reactions ($k = 10^3$–10^5 M^{-1} s^{-1}), thus the **IP-C2$^{\bullet}$** may also contribute to the propagation reactions. However, in the **TL** solution, the **NVP** + **TBO$^{\bullet}$/CMO$^{\bullet}$** reactions were about 10^3–10^4 times faster than the **NVP** + **TL-C7$^{\bullet}$** reaction.

The AIM analysis (Table S1, Fig. S2, ESI†) indicated that energies (E_{H-B}) of the C7⋯C/O intermolecular contacts of RAF transition states are in the range of −13.1 to −9.8 kcal mol^{-1}. The replacement of the methyl group at **TBO$^{\bullet}$** by phenyl at **CMO$^{\bullet}$** could reduce the E_{H-B}(C7⋯O) values, particularly in **TL** solvent. That may be a reason for the high rate constant of the **CMO$^{\bullet}$** + **NVP** reaction.

3.2 The propagation reaction

As previously mentioned, the main intermediates of the radical process were **IP-C2-C7-NVP**, **TL-C7-C7-NVP**, **TBO-C7-NVP**, and **CMO-C7-NVP** (Table 3 and Fig. 3). These radicals were thought to follow the RAF pathway, the basic reaction mechanism of radical chain polymerization, and react with **NVP** at the most active site (C7). Thus, using the QM-ORSA approach,[33] the propagation rate constant (k_p) of the reaction between **IP-C2-C7-NVP/TL-C7-C7-NVP/TBO-C7-NVP/CMO-C7-NVP** and **NVP** was determined. The results are provided in Table 4, and the TSs are illustrated in Fig. 5.

As shown in Tables 4, in the **IP** solution, the k_p value of the **IP-C2-C7-NVP** + **NVP** reaction ($k_p = 1.20 \times 10^3$ M^{-1} s^{-1}) was similar to that of the **TBO-C7-NVP** + **NVP** reaction ($k_p = 2.10 \times 10^3$ M^{-1} s^{-1}), whereas these values were about 36.4 and 63.6 (for **IP-C2-C7-NVP** and **TBO-C7-NVP**, respectively) times higher than that of the **CMO-C7-NVP** + **NVP** reaction ($k_p = 3.30 \times 10^1$ M^{-1}

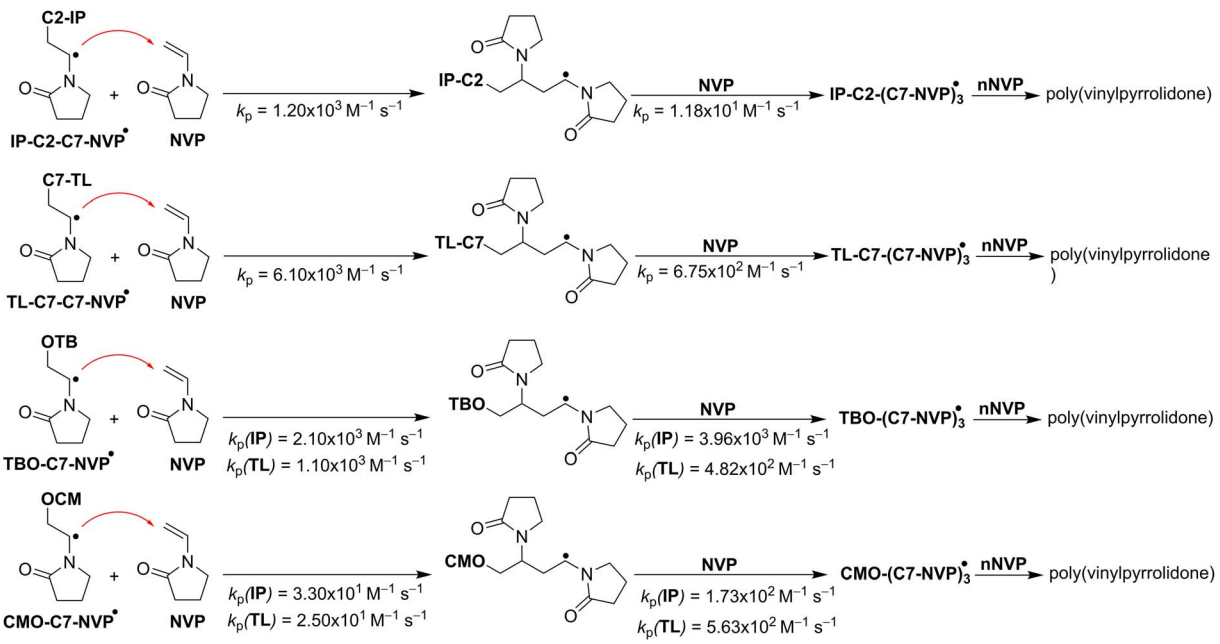

Fig. 5 The propagation reactions.

© 2023 The Author(s). Published by the Royal Society of Chemistry

Open Access Article. Published on 04 August 2023. Downloaded on 2/16/2026 2:18:28 AM. This article is licensed under a Creative Commons Attribution 3.0 Unported Licence.

s^{-1}). Therefore, the radical polymerization of **NVP** in the isopropanol solution with $(\mathbf{CMO})_2$ as an initiator could produce **PVP** with a solvent molecule (**IP-C2**). That is in good agreement with the experimental data.[4] However, when $(\mathbf{TBO})_2$ is used as an initiator, the **PVP** may contain both the solvent (**IP**) and initiator (**TB**) structures.

A similar trend was also observed in the **TL** solvent, the **TL-C7-C7-NVP**/**TBO-C7-NVP** + **NVP** reactions were about 24.4 (k_p = 6.10 × 10^3 M^{-1} s^{-1}) and 4.4 (k_p = 1.10 × 10^3 M^{-1} s^{-1}) times faster than the **CMO-C7-NVP** + **NVP** reaction (k_p = 2.50 × 10^1 M^{-1} s^{-1}), respectively. Being the solvent, the amount of **TL** is significantly greater than that of the initiators, *i.e.* $(\mathbf{TBO})_2$ or $(\mathbf{CMO})_2$, thus the **PVP** produced this way could contain residues of both the solvent (**TL**) and initiators (**TB**, **CM**), despite the rate constant of the **TL-C7˙** + **NVP** reaction being lower than those of the **TBO˙**/**CMO˙** + **NVP** reactions (Table 3).

The investigation of the chain extension (adding the second **NVP** molecule) revealed that the k_p values ($k_p = 10^1$–10^2 M^{-1} s^{-1}, Table 4, Fig. 3 and 5) were comparable to those of the initial propagation reactions. It appears that the rate constants of the propagation reactions are in the range of 10^1–10^3 M^{-1} s^{-1}, depending on the performed radicals and solvents.

Since the atoms adjacent to the center of the radicals are identical, the propagation rate constants of **CMO-C7-NVP** + **NVP** in both **IP** and **TL** were found to be lower than those of other propagation reactions. However, the k_p values for the **CMO-C7-NVP-C7-NVP** + **NVP** were fairly similar to those of the **TBO-C7-NVP-C7-NVP** + **NVP** reactions. This could be due to the steric effects of **CMO** in the **CMO-C7-NVP** + **NVP** reaction.[60]

4. Conclusion

Using computational chemistry, the mechanism and kinetics of the alkoxy radical polymerization of *N*-vinylpyrrolidone in organic solvents, namely isopropanol, and toluene, have been successfully determined. It was discovered that both solvents, *i.e.* isopropanol and toluene could contribute to the initiation reactions alongside the initiator radicals **TBO˙** and **CMO˙**. The rate constant varied as a function of the initiators and solvents used. The values of the constant rate of propagation were approximately 10^1–10^3 M^{-1} s^{-1}. In all of the analyzed organic solvents, the radical polymerization of **NVP** with $(\mathbf{CMO})_2$ as an initiator occurred fairly similarly with $(\mathbf{TBO})_2$, whereas the solvents could contribute to the radical polymerization of **NVP**.

Author contributions

Quan V. Vo: conceptualization, methodology, investigation, formal analysis, funding acquisition, writing – original draft, supervision. Truong Le Bich Tram, Hoang Phuoc Loc, Nguyen Thi Hoa: formal analysis, data curation, investigation, visualization, writing – original draft. Adam Mechler: project supervision, administration, software, writing – review & editing.

Conflicts of interest

There are no conflicts to declare.

Acknowledgements

This research is funded by the Vietnamese Ministry of Education and Training under project number B2021-DNA-18 (T. L. B. T.).

References

1 M. Kurakula and G. K. Rao, *J. Drug Delivery Sci. Technol.*, 2020, **60**, 102046.
2 M. Teodorescu and M. Bercea, *Polym.-Plast. Technol. Eng.*, 2015, **54**, 923–943.
3 Y. Luo, Y. Hong, L. Shen, F. Wu and X. Lin, *AAPS PharmSciTech*, 2021, **22**, 1–16.
4 F. Haaf, A. Sanner and F. Straub, *Polym. J.*, 1985, **17**, 143–152.
5 R. Awasthi, S. Manchanda, P. Das, V. Velu, H. Malipeddi, K. Pabreja, T. D. Pinto, G. Gupta and K. Dua, in *Engineering of Biomaterials for Drug Delivery Systems*, Elsevier, 2018, pp. 255–272.
6 J.-C. An, A. Weaver, B. Kim, A. Barkatt, D. Poster, W. N. Vreeland, J. Silverman and M. Al-Sheikhly, *Polymer*, 2011, **52**, 5746–5755.
7 A. Davison, D. Sangster, J. Lynn and E. Senogles, *J. Polym. Sci.*, 1976, 249–257.
8 J. Davis, D. Sangster and E. Senogles, *Aust. J. Chem.*, 1981, **34**, 1423–1431.
9 C. Dispenza, M. A. Sabatino, N. Grimaldi, B. Dahlgren, M. Al-Sheikhly, J. F. Wishart, Z. Tsinas, D. L. Poster and M. Jonsson, *Radiat. Phys. Chem.*, 2020, **174**, 108900.
10 N. Bartoszek, P. Ulański and J. M. Rosiak, *Int. J. Chem. Kinet.*, 2011, **43**, 474–481.
11 P. Sawicki, G. Łapienis, S. Kadłubowski, P. Ulański and J. M. Rosiak, *Radiat. Phys. Chem.*, 2023, **202**, 110543.
12 K. M. Koczkur, S. Mourdikoudis, L. Polavarapu and S. E. Skrabalak, *Dalton Trans.*, 2015, **44**, 17883–17905.
13 G. Ghosh, M. K. Naskar, A. Patra and M. Chatterjee, *Opt. Mater.*, 2006, **28**, 1047–1053.
14 R. Singh and D. Singh, *J. Mater. Sci.: Mater. Med.*, 2012, **23**, 2649–2658.
15 M. Wang, L. Xu, H. Hu, M. Zhai, J. Peng, Y. Nho, J. Li and G. Wei, *Nucl. Instrum. Methods Phys. Res., Sect. B*, 2007, **265**, 385–389.
16 Q. V. Vo, T. L. B. Tram, N. T. Hoa, A. N. Au-Duong and A. Mechler, *Polym. Degrad. Stab.*, 2023, **216**, 110483.
17 A. Galano and J. Raúl Alvarez-Idaboy, *Int. J. Quantum Chem.*, 2019, **119**, e25665.
18 B. H. Northrop and R. N. Coffey, *J. Am. Chem. Soc.*, 2012, **134**, 13804–13817.
19 V. Fındık, I. Degirmenci, Ş. Çatak and V. Aviyente, *Eur. Polym. J.*, 2019, **110**, 211–220.
20 E. Frick, C. Schweigert, B. B. Noble, H. A. Ernst, A. Lauer, Y. Liang, D. Voll, M. L. Coote, A.-N. Unterreiner and C. Barner-Kowollik, *Macromolecules*, 2016, **49**, 80–89.
21 I. Degirmenci, S. u. k. Eren, V. Aviyente, B. De Sterck, K. Hemelsoet, V. Van Speybroeck and M. Waroquier, *Macromolecules*, 2010, **43**, 5602–5610.
22 T. Furuncuoglu, I. Ugur, I. Degirmenci and V. Aviyente, *Macromolecules*, 2010, **43**, 1823–1835.

© 2023 The Author(s). Published by the Royal Society of Chemistry

Open Access Article. Published on 04 August 2023. Downloaded on 2/16/2026 2:18:28 AM. This article is licensed under a Creative Commons Attribution 3.0 Unported Licence.

23 P. Deglmann, I. Müller, F. Becker, A. Schäfer, K. D. Hungenberg and H. Weiß, *Macromol. React. Eng.*, 2009, **3**, 496–515.
24 C. Y. Lin, E. I. Izgorodina and M. L. Coote, *Macromolecules*, 2010, **43**, 553–560.
25 P. Deglmann, K. D. Hungenberg and H. M. Vale, *Macromol. React. Eng.*, 2017, **11**, 1600037.
26 P. Deglmann, K. D. Hungenberg and H. M. Vale, *Macromol. React. Eng.*, 2018, **12**, 1800010.
27 M. Dossi, G. Storti and D. Moscatelli, *Macromol. Theory Simul.*, 2010, **19**, 170–178.
28 E. Mavroudakis, D. Cuccato and D. Moscatelli, *Polymers*, 2015, **7**, 1789–1819.
29 J. A. Kretzmann, D. Ho, C. W. Evans, J. H. Plani-Lam, B. Garcia-Bloj, A. E. Mohamed, M. L. O'Mara, E. Ford, D. E. Tan and R. Lister, *Chem. Sci.*, 2017, **8**, 2923–2930.
30 M. D. Nothling, Z. Xiao, N. S. Hill, M. T. Blyth, A. Bhaskaran, M. A. Sani, A. Espinosa-Gomez, K. Ngov, J. White and T. Buscher, *Sci. Adv.*, 2020, **6**, eaaz0404.
31 A. Galano and J. R. Alvarez-Idaboy, *J. Comput. Chem.*, 2013, **34**, 2430–2445.
32 Q. V. Vo, N. T. Hoa and A. Mechler, *Polym. Degrad. Stab.*, 2021, **185**, 109483.
33 M. E. Alberto, N. Russo, A. Grand and A. Galano, *Phys. Chem. Chem. Phys.*, 2013, **15**, 4642–4650.
34 N. T. Hoa and Q. V. Vo, *Chemosphere*, 2023, **314**, 137682.
35 M. G. Evans and M. Polanyi, *Trans. Faraday Soc.*, 1935, **31**, 875–894.
36 H. Eyring, *J. Chem. Phys.*, 1935, **3**, 107–115.
37 D. G. Truhlar, W. L. Hase and J. T. Hynes, *J. Phys. Chem.*, 1983, **87**, 2664–2682.
38 E. Dzib, J. L. Cabellos, F. Ortíz-Chi, S. Pan, A. Galano and G. Merino, *Int. J. Quantum Chem.*, 2019, **119**, e25686.
39 E. Dzib, J. L. Cabellos, F. Ortiz-Chi, S. Pan, A. Galano and G. Merino, *Eyringpy 1.0.2*, Cinvestav, Mérida, Yucatán, 2018.
40 E. Pollak and P. Pechukas, *J. Am. Chem. Soc.*, 1978, **100**, 2984–2991.
41 A. Fernández-Ramos, B. A. Ellingson, R. Meana-Pañeda, J. M. Marques and D. G. Truhlar, *Theor. Chem. Acc.*, 2007, **118**, 813–826.
42 C. Eckart, *Phys. Rev.*, 1930, **35**, 1303.
43 F. C. Collins and G. E. Kimball, *J. Colloid Sci.*, 1949, **4**, 425–437.
44 M. Von Smoluchowski, *Z. Phys. Chem.*, 1917, **92**, 129–168.
45 D. G. Truhlar, *J. Chem. Educ.*, 1985, **62**, 104.
46 A. Einstein, *Ann. Phys.*, 1905, **17**, 549–560.
47 G. G. Stokes, *Mathematical and Physical Papers*, University Press, Cambridge, 1905.
48 M. J. Frisch, G. W. Trucks, H. B. Schlegel, G. E. Scuseria, M. A. Robb, J. R. Cheeseman, G. Scalmani, V. Barone, B. Mennucci, G. A. Petersson, H. Nakatsuji, M. Caricato, X. Li, H. P. Hratchian, A. F. Izmaylov, G. Z. J. Bloino, J. L. Sonnenberg, M. Hada, M. Ehara, K. Toyota, R. Fukuda, J. Hasegawa, M. Ishida, T. Nakajima, Y. Honda, O. Kitao, H. Nakai, T. Vreven, J. A. Montgomery Jr, J. E. Peralta, F. Ogliaro, M. Bearpark, J. J. Heyd, E. Brothers, K. N. Kudin, V. N. Staroverov, T. Keith, R. Kobayashi, J. Normand, K. Raghavachari, A. Rendell, J. C. Burant, S. S. Iyengar, J. Tomasi, M. Cossi, N. Rega, J. M. Millam, M. Klene, J. E. Knox, J. B. Cross, V. Bakken, C. Adamo, J. Jaramillo, R. Gomperts, R. E. Stratmann, O. Yazyev, A. J. Austin, R. Cammi, C. Pomelli, J. W. Ochterski, R. L. Martin, K. Morokuma, V. G. Zakrzewski, G. A. Voth, P. Salvador, J. J. Dannenberg, S. Dapprich, A. D. Daniels, O. Farkas, J. B. Foresman, J. V. Ortiz, J. Cioslowski and D. J. Fox, *Gaussian 16, Revision B.01*, Gaussian, Inc., Wallingford CT, 2016.
49 M. Carreon-Gonzalez, A. Vivier-Bunge and J. R. Alvarez-Idaboy, *J. Comput. Chem.*, 2019, **24**, 2103–2110.
50 Y. Zhao, N. E. Schultz and D. G. Truhlar, *J. Chem. Theory Comput.*, 2006, **2**, 364–382.
51 A. Galano and J. R. Alvarez-Idaboy, *J. Comput. Chem.*, 2014, **35**, 2019–2026.
52 Y. Zhao and D. G. Truhlar, *Theor. Chem. Acc.*, 2008, **120**, 215–241.
53 A. K. Chandra, P.-C. Nam and M. T. Nguyen, *J. Phys. Chem. A*, 2003, **107**, 9182–9188.
54 C. Iuga, J. R. l. Alvarez-Idaboy and N. Russo, *J. Org. Chem.*, 2012, **77**, 3868–3877.
55 Q. V. Vo, M. V. Bay, P. C. Nam and A. Mechler, *J. Phys. Chem. B*, 2019, **123**, 7777–7784.
56 Q. V. Vo, M. V. Bay, P. C. Nam, D. T. Quang, M. Flavel, N. T. Hoa and A. Mechler, *J. Org. Chem.*, 2020, **85**, 15514–15520.
57 A. V. Marenich, C. J. Cramer and D. G. Truhlar, *J. Phys. Chem. B*, 2009, **113**, 6378–6396.
58 F. Biegler-König, *AIM 2000*, University of Applied Sciences, Bielefeld, Germany, 2000.
59 R. F. Bader, *Chem. Rev.*, 1991, **91**, 893–928.
60 H. Fischer and L. Radom, *Angew. Chem., Int. Ed.*, 2001, **40**, 1340–1371.

© 2023 The Author(s). Published by the Royal Society of Chemistry